Journal of Aerosol Science 150 (2020) 105643

Contents lists available at ScienceDirect

Journal of Aerosol Science

journal homepage: http://www.elsevier.com/locate/jaerosci

Aerosol analysis using quantum cascade laser infrared spectroscopy: Application to crystalline silica measurement☆

Shijun Wei [a,b], Pramod Kulkarni [a,*], Lina Zheng [c], Kevin Ashley [d]

[a] Centers for Disease Control and Prevention, National Institute for Occupational Safety and Health, Cincinnati, OH, 45226, USA
[b] University of Cincinnati, Department of Mechanical and Materials Engineering, Cincinnati, OH, 45221, USA
[c] Department of Industrial Hygiene Engineering, School of Safety Engineering, China University of Mining and Technology, Xuzhou, 221116, Jiangsu, PR China
[d] Ashley Analytical Associates, 1921 West Eagle Way, Amado, AZ, 85645, USA

ARTICLE INFO

Keywords:
Quantum cascade laser
Infrared spectroscopy
Crystalline silica aerosol

ABSTRACT

A method for trace analysis of aerosol mineral components using quantum cascade laser (QCL) based infrared absorption spectroscopy is described. The measurement approach involves: (a) collection of aerosol on a particulate filter; (b) sample treatment using low-temperature oxygenated plasma to minimize the matrix interferences; (c) redeposition of the treated sample as a dried spot for direct-on-filter analysis; and (d) infrared transmittance measurement of the dried spot using the QCL and mercury-cadmium-telluride detector. The method was applied to quantification of trace α-quartz in workplace aerosols. Infrared absorbance spectra in the range 750–1030 cm^{-1} were obtained using the QCL instrument; the characteristic peak of α-quartz at 798 cm^{-1} was used to measure its content. A correction scheme was applied to account for spectral interference from kaolinite mineral for coal dust samples. The detection limit for α-quartz was estimated to be 0.12 μg for a dried spot diameter of 1 mm. This detection limit is an order-of-magnitude lower than those attainable by the current standard X-ray diffraction (XRD) or Fourier transform infrared spectroscopy (FTIR) methods involving similar sample preparation and treatment. The QCL method was extended to the measurement of respirable α-quartz concentrations in workplace aerosols released during cutting of fiber-reinforced cement and engineered stone products (used in building construction), as well as those from various coal mine dusts. The measurements compared well with those from the standard XRD method, even for samples with matrix and mineral interferences. The results show that QCL-based IR transmission spectroscopy can offer sensitive, trace-level measurement of aerosol mineral components.

1. Introduction

Exposure to crystalline silica aerosol in the respirable size range, often referred to as respirable crystalline silica (RCS), is common in many mining and industrial environments involving production, manufacturing, and handling of silica-containing materials and

☆ Disclaimer—The findings and conclusions in this report are those of the authors and do not necessarily represent the views of the National Institute for Occupational Safety and Health. Mention of product or company name does not constitute endorsement by the Centers for Disease Control and Prevention.

* Corresponding author.
E-mail address: PSKulkarni@cdc.gov (P. Kulkarni).

https://doi.org/10.1016/j.jaerosci.2020.105643
Received 12 May 2020; Received in revised form 3 August 2020; Accepted 4 August 2020
Available online 23 August 2020
0021-8502/Published by Elsevier Ltd.

minerals (MSHA, 2013; NIOSH, 2017b). Inhalation of RCS can lead to silicosis and lung cancer, and has also been linked to chronic obstructive pulmonary disease, kidney disease, and autoimmune disorder (MSHA, 2013; NIOSH, 2017b). More than two million workers in the Unites States are exposed to RCS across various industries (Yassin, Yebesi, & Tingle, 2005). RCS appears typically in the form of α-quartz (and/or less commonly, as cristobalite) in most workplaces (NIOSH, 2017b). Numerous epidemiologic studies indicate that occupational exposure limits (OELs) for RCS are not sufficiently protective to prevent chronic silicosis (International Organization for Standardization, 2015; NIOSH, 2017b; Esswein, Breitenstein, Snawder, Kiefer, & Sieber, 2013). The U.S. Occupational Safety and Health Administration (OSHA) has recently promulgated a lower permissible exposure limit (PEL) for RCS of 50 μg m^{-3} averaged over an 8-hour work shift to further reduce health risks from silica exposure (OSHA, 2016). Other OELs for RCS are yet lower than the OSHA PEL (IFA, 2018). Increasingly, sensitive methods are needed to allow for trace measurement of airborne RCS.

Established methods for quantification of airborne RCS entail collection of workplace aerosols on a filter media, which is subsequently analyzed in the laboratory using analytical methods employing either X-ray diffraction (XRD) (International Organization for Standardization, 2015) or Fourier transform infrared (FTIR) spectroscopy (ASTM, 2014;HSE, 2014). Sample preparation schemes involving plasma ashing or muffle furnace treatment are usually employed to mitigate matrix interferences (ASTM, 2014; International Organization for Standardization, 2015). Limits of detection (LODs) for respirable quartz obtained by these standard XRD and FTIR methods range from 3 to 10 μg per sample (HSE, 2014,pp. 1–21; NIOSH, 2017b). While these methods allow measuring reliably at the PEL when sampled air volume is about 1 m^3 or more (typically a full shift/8-hr sample), the precision is poorer for task specific, short term measurements (when the sampled air volume is much lower than 1 m^3). For demonstration of effective exposure mitigation and meaningful exposure measurement of RCS, development of more sensitive in-field, field-portable, and laboratory methods are critically needed.

To address these needs, in this study a new approach involving infrared (IR) transmission spectroscopy using a quantum cascade laser (QCL) is employed as a sensitive method for aerosol analysis. The methodology allows analysis of aerosol samples collected using a variety of air sampling devices and filter media. The procedure also incorporates filter pretreatment to enable trace analysis of samples with potentially complex matrix and spectral interferences. In a previous proof-of-concept study (Wei, Kulkarni, Ashley, & Zheng, 2017), we demonstrated the utility of QCL for measurement of α-quartz in certified reference materials. We showed that when the particulate sample is concentrated as a small deposit, superior detection limits could be achieved (Wei et al., 2017). In this study, we extend the same spectroscopic approach to analysis of real-world aerosols from workplace atmospheres. Unlike our previous study (Wei et al., 2017), which required direct collection of particles from air as a small spot, the method presented here allows analysis of filter samples collected using conventional air sampling methodologies.

2. Methods

The overall measurement scheme used in this study (Wei et al., 2017), shown in Fig. 1, involves the following steps: i) collection of respirable airborne particles on a filter medium using a size-selective sampling device; ii) filter pre-treatment using low-temperature ashing in an oxygen plasma; iii) sample resuspension in a solvent, followed by redeposition on a filter substrate as a concentrated spot; and iv) analysis of redeposited spot (after drying) using QCL-IR spectroscopy.

2.1. Air sampling

Test atmospheres or calibration aerosols containing RCS were generated to produce stable air concentrations by using a fluidized bed aerosol generator (Model 3400A; TSI Inc., Shoreview, MN, USA) operated at 9 L min^{-1}. 25-mm diameter Mixed Cellulose Ester (MCE; 0.8 μm pore size) filters housed in 25-mm filter cassettes (SKC Inc., Eighty Four, PA, USA) were used to collect the particulate matter samples. The particulate samples were collected onto the filters using a respirable cyclone inlet (GK 2.69; Mesa laboratories Inc) directly from the aerosol phase at a flow rate of 2 **L** $\mathbf{MIN}^{-1}$ using battery-powered personal air sampling pumps (GilAir Plus, Sensidyne, St. Petersburg, FL, USA).

The mass concentrations of the test aerosol were measured at the outlet of the fluidized bed aerosol generator using an optical

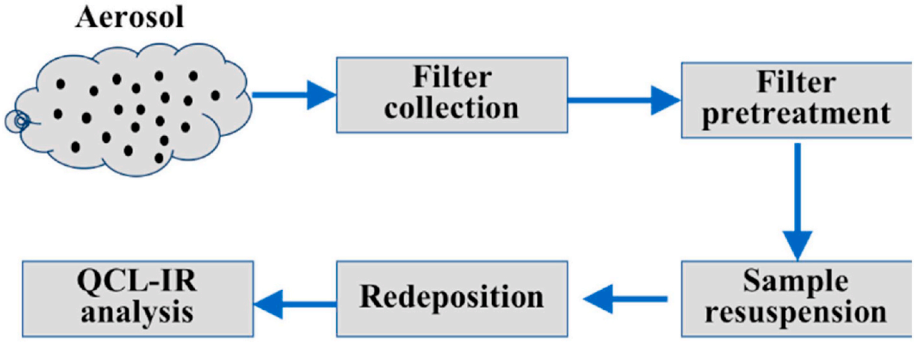

Fig. 1. A schematic diagram of aerosol measurement using QCL-IR spectroscopy.

photometer (DustTrak™; Model 8533, TSI Inc., Shoreview, MN, USA). The DustTrak™ was calibrated with respect to gravimetric measurements (to ± 1 μg) using the same test/calibration aerosol to allow accurate estimation of filter mass loadings.

2.2. Sample pretreatment

The MCE filter samples containing collected respirable airborne particles were placed in 25-mL borosilicate glass vials (PCM Surplus World, St-Laurent, PQ, Canada). A low-temperature plasma asher (Series 600, Anatech, Union City, CA, USA) was used to ash the filters in accordance with standardized methods (ASTM, 2014; NIOSH, 2017b). The plasma asher was operated at 50 mL min^{-1} oxygen flow rate and 250 W power for 90 min to ensure decomposition of the entire filter matrix, with only the particulate sample remaining for further resuspension and redeposition. After completion of ashing, 2 mL of ultra-filtered (18 MΩ-cm) deionized (DI) water (ThermoFisher, Rochester, NY, USA) was added to the vials. Then each vial was sonicated for 5 min in an ultrasonic bath prior to the liquid suspension being transferred into a 10-mL polytetrafluoroethylene (PTFE) filtration syringe with a Luer-lok™ tip (Becton Dickinson, Franklin Lakes, NJ. USA). Each vial was subsequently rinsed with 1 mL DI water to ensure resuspension of aerosol particles. From each vial, a 3-mL suspension was transferred into a PTFE filtration syringe.

2.3. Sample resuspension and redeposition

The apparatus for redeposition of the analyte suspension as a concentrated spot (which is subsequently dried and analyzed by QCL-IR) has been previously described in Figs. 1 and 2 (Wei et al., 2017). As presented in detail elsewhere (Zheng, Kulkarni, Birch, Ashley, & Wei, 2018), two 3D-printed masking orifice plates were housed in a 13-mm diameter stainless steel syringe filter holder (EMD Millipore, Darmstadt, Germany) with a Luer-lok™ fitting. A 13-mm diameter, 0.8 μm pore size polycarbonate (PC) membrane filter (GVS Life Sciences, Morecambe, UK) was placed between two masking orifice plates. Three pairs of masking orifice plates with different orifice diameters (1.0, 1.5 and 3.0 mm) were designed to yield different sample spot sizes. A 10-mL syringe filled with the analyte suspension was securely attached to the syringe filter holder, and the liquid suspension containing the treated sample was then pushed through the orifice. The diameters of the filtered deposition areas were the same as those of the orifices of the masking plates (Wei et al., 2017).

2.4. QCL-IR instrument setup

QCL-IR transmission spectroscopy was used for quantitative measurement of respirable α-quartz in the treated samples. The QCL-IR instrument setup used in this work has been described earlier (Wei et al., 2017). Briefly, the IR laser beam from the QCL source was focused onto the particulate sample deposited on the PC membrane filter, and the transmitted IR radiation was measured using a mercury-cadmium-telluride (MCT) detector (Block Engineering, Southborough, MA, USA). The QCL-IR system was customized to provide spectra in the frequency range of 750–1030 cm^{-1} with a wavenumber resolution of 2 cm^{-1}. The characteristic peak of α-quartz

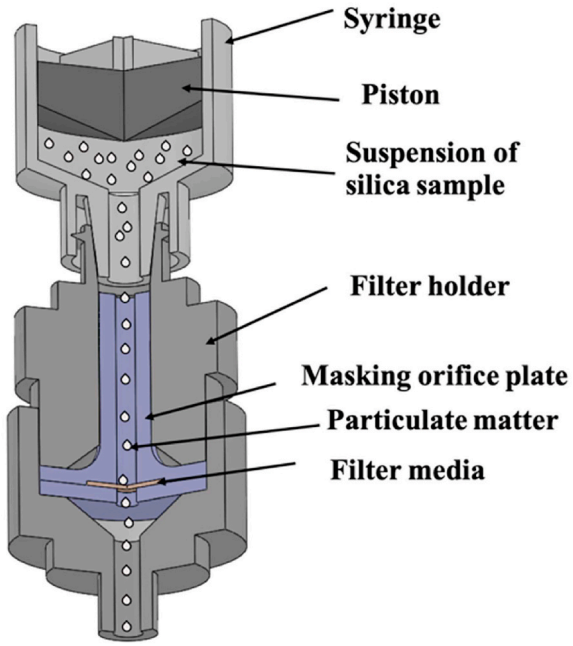

Fig. 2. A cross-sectional view of the apparatus used for obtaining dried spot through redeposition of the analyte suspension using syringe filtration.

is a doublet at 780 cm^{-1} and 798 cm^{-1}; the peak of greater intensity at 798 cm^{-1} was used for quantification of α-quartz (ASTM, 2014).

2.5. Calibration

For calibration, suspensions of Standard Reference Material (SRM) respirable α-quartz (SRM 1878a; NIST, Gaithersburg, MD, USA), with various colloidal concentration levels ranging from 0.1 to 100 μg mL^{-1}, were prepared in ultra-filtered DI water. Each suspension was agitated and mixed for 10–20 s using a vortex mixer (Barnstead Thermolyne Maxi-Mix Plus, Model# M63215, Ramsey, MN, USA). 2 mL of each suspension was deposited onto a PC filter using the redeposition apparatus described previously (Wei et al., 2017). The filters were air dried to yield dried spot samples for QCL analysis.

In order to obtain a superior signal-to-noise ratio, detector integration time and spectral averaging were optimized. An integration time of 3 s per scan was used, and each spectrum comprised an average of 16 repeat scans. A representative spectrum for each sample was obtained by averaging three spectra collected from three randomly selected locations on the particulate sample spot. A blank spectrum was obtained using a blank filter media (identical to that used for sample collection; however, with no analyte on it). Blank measurement was identical to sample measurement in all respects, except for the absence of the analyte. Transmittance of the sample filter (containing the analyte) was divided by the transmittance of the blank filter to obtain a normalized transmittance spectrum, which was further converted to a normalized absorbance spectrum. This ratioing procedure ensured that IR absorption spectrum reflected only the analyte absorbance. All absorption spectra in this work were obtained using this procedure.

Both multivariate and univariate approaches were used for constructing calibration models. A multivariate technique using partial least squares (PLS) regression (Valderrama, Braga, & Poppi, 2007) was applied to quantify the content of RCS (as α-quartz) in the particulate samples, as described previously (Wei et al., 2017). The PLS model involves linear regression between explanatory variables X (i.e., absorbance data from QCL-IR) and response variables Y (i.e., α-quartz mass in the particulate spot samples).

Univariate calibration curves were also constructed by plotting the peak height at 798 cm^{-1} as a function of the α-quartz mass. The peak height was calculated using the difference between the baseline absorbance and the peak absorbance at 798 cm^{-1}. The baseline was obtained by drawing a linear curve between the absorbance values at 766 cm^{-1} and 842 cm^{-1}.

2.6. Workplace aerosol samples

Real-world aerosols from various industrial workplaces containing α-quartz were used to evaluate the effectiveness of the QCL method. Three types of workplace samples, representing three distinct particulate matrices and corresponding interferences, were prepared for validation of the procedure. Filter samples of these three types of workplace respirable aerosols were obtained in the laboratory by re-aerosolizing the actual dust collected in various workplaces. This was necessary in order to obtain filters with well-defined mass loadings under well-controlled conditions in the laboratory.

Aerosols were generated by re-aerosolizing the powders containing fine particles produced during cutting of silicate materials (such as engineered stone countertop and fiber-reinforced cement siding) at construction sites.

Engineered stone (ST) sample was collected during cutting of a thick engineered stone slab (e.g. Corian®) using a powered circular saw at a stone countertop fabrication facility. This sample matrix contained approximately 90% α-quartz, with the remaining matrix containing resins, polymers, and pigments.

Fiber cement (FC) siding sample, obtained from fiber-reinforced cement composite siding, was collected during its cutting operation using a power saw tool at a construction site. Sample FC contained relatively small amounts of α-quartz ranging from 10 to 30%, along with other matrix components such as cellulose fibers and hydraulic cement binder.

Coal dust (CD) samples were prepared by re-aerosolizing the dust from representative crushed coal materials obtained from the Penn State Coal Sample Bank (PSCB; Energy Institute, University Park, PA, USA). Table 1 describes the chemical constituents of the CD samples. The oxide composition of CD samples is based on the analysis of high-temperature ash (HTA). The PSCB samples were collected directly from bituminous coal mining sites after further grinding of the coarse dust particles. The fraction of α-quartz was estimated to be approximately 5–20%.

2.7. Kaolinite

Kaolinite (Sigma-Aldrich, St. Louis, MO, USA) suspensions were prepared with different concentrations ranging from 1 to 5 μg·mL^{-1}. 2 mL of each suspension was redeposited as a 1.5 mm spot on a 25-mm MCE filter using the orifice-assisted syringe filtration apparatus described above.

Table 1
Details of coal mine dust samples obtained from the Penn State Coal Sample Bank.

Sample#	PSCB Sample	Origin of coal mine	Major oxides, % of High-Temperature Ash (HTA)		
			SiO_2	Al_2O_3	Fe_2O_3
1	DECS-12	Greene County, PA, USA	55.8	25.8	6.37
2	DECS-22	Armstrong County, PA, USA	62	23.2	8.7
3	DECS-32	Kanawha County, WV, USA	51	34.3	3.15
4	DECS-34	Washington County, PA, USA	48.5	23.2	14.84

3. Results and discussions

3.1. Sample recovery

We investigated recovery of α-quartz during sample pre-treatment with low-temperature plasma ashing using NIST SRM 1878a. Aqueous suspensions of this SRM were prepared at three concentrations: 2, 5, and 10 μg μL $^{-1}$. Aliquots of 10 μL of each suspension were transferred using a pipette to 25-mm MCE filters; three replicates were prepared for each mass loading. Recoveries were found to be 91%, 94%, and 93% for 20, 50 and 100 μg filter mass loading, respectively. Based on these measurements, a mean recovery of 92% was used to retrieve analyte content from the QCL-IR measurements. This recovery is comparable to recoveries using the low-temperature plasma ashing reported in previous studies (Lee, Van Orden, Cox, Arlauckas, & Kautz, 2016).

3.2. QCL-IR spectra of NIST SRM samples

Fig. 3 Shows the QCL-IR spectra for NIST SRM 1878asamples with various α-quartz mass loadings using deposition diameter of 1.0,

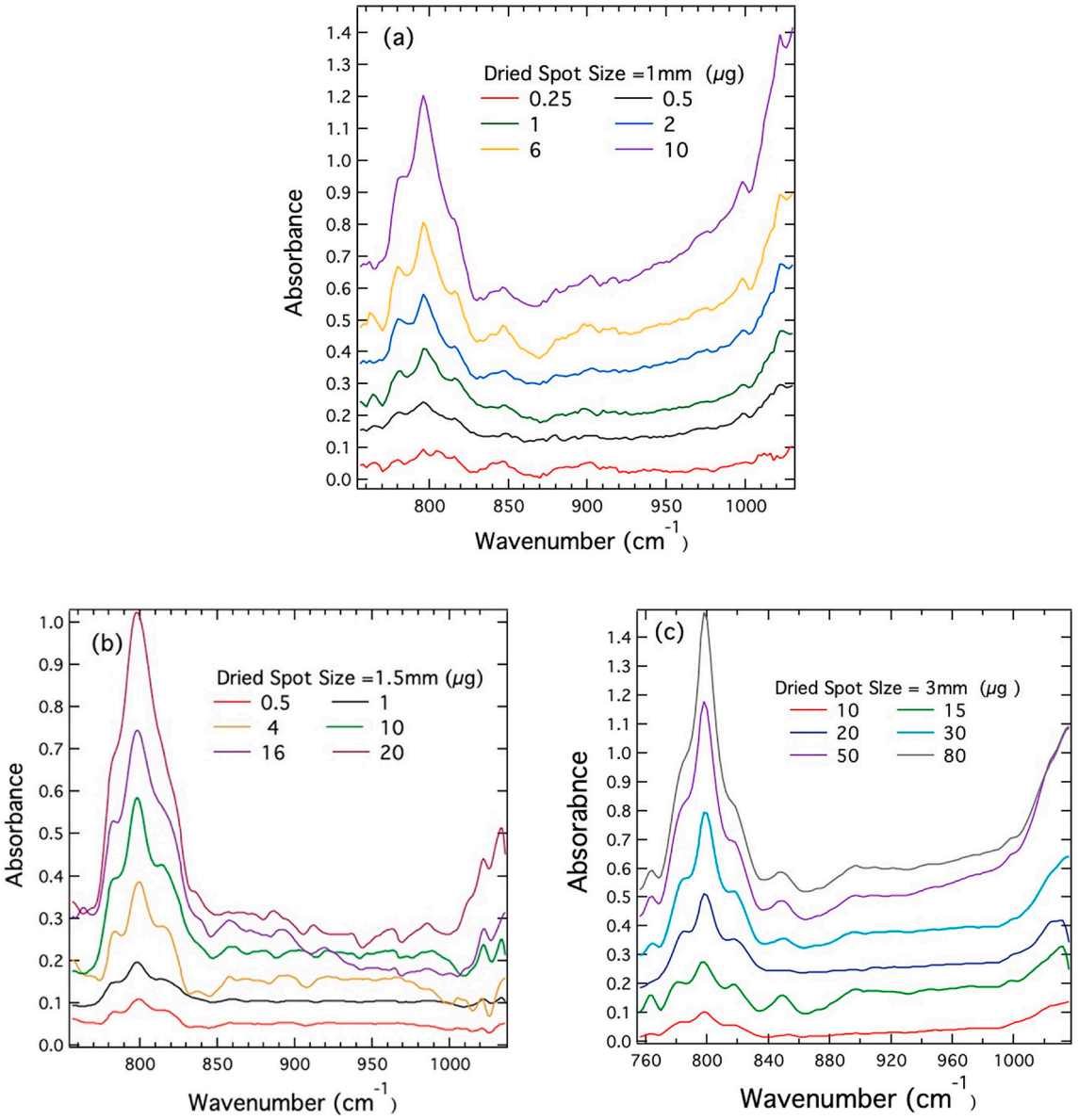

Fig. 3. QCL-IR spectra of SRM samples with various α-quartz mass loadings per filter with dried spot diameter of: (a) 1, (b) 1.5, and (c) 3 mm, respectively.

1.5, and 3.0 mm, respectively. For each mass loading, three replicates sample filters were prepared for QCL-IR measurement. The total mass loadings of α-quartz were in the range 0.25–10 μg, 0.5–20 μg, and 10–100 μg, corresponding to the three different spot diameters, respectively. For each deposition diameter, the peak absorbance at 798 cm^{-1} decreases with increasing α-quartz mass loading. The results show a strong correlation between the absorbance signal from QCL measurement and the mass loading for a specific spot diameter. These spectra were then used to construct a PLS calibration model and univariate calibration model for predicting α-quartz mass loading.

3.3. Univariate calibration

Fig. 4(a) shows three univariate calibration curves constructed for 1.0, 1.5- and 3.0-mm diameter dried spots, respectively, using total mass per spot (or filter). The slope of the calibration curve decreases with increasing diameter of dried spot: the slopes of calibration curves for 1.0, 1.5, and 3.0 mm spots are 0.11, 0.05 and 0.01, respectively. The R^2 values of linear regression were 0.98, 0.99, 0.98 respectively. Fig. 4(b) shows the corresponding calibration curve plotted as a function of analyte mass density, defined as analyte mass per unit area of the dried spot. The sample spot area was assumed to be the same as the orifice size of the masking orifice. Plotting calibration curves with respect to mass density allows combining all absorbance measurements (obtained from different sample spot sizes) into one curve. Thus three calibration curves are reduced to one universal curve when plotted as a function of surface mass density. The slope of the universal calibration curve is 1.37 with $R^2 = 0.88$. Error bars around each data point in Fig. 4 Represent standard deviations about the means for at least 3 replicate measurements. The shaded region represents the 95% confidence limit about the combined calibration curve.

3.4. Multivariate calibration

As demonstrated in Fig. 5(a)-(b), in constructing a partial least squares (PLS) model, the absorbance data in the wavenumber range 766–842 cm^{-1} were selected as X variables, and mass loadings of 57 filter samples (ranging from 0.25 to 100 μg) were used as Y variables. The PLS model was constructed using the procedure outlined in our previous study (Wei et al., 2017). The spectral data were pre-processed using an auto-scaling and mean-centering method. Two latent variables were used that explained more than 90% of the variance in the data. 'Leave-one-out' cross validation method was used to evaluate the performance of the PLS model. Almost all the predicted mass loadings were within the 95% confidence limit; the regression coefficient R^2 was 0.98. For the predicted vs. measured α-quartz mass density (analyte mass per unit area of dried spot) obtained using the PLS model, most data points fell within the 95% confidence limit; the R^2 value was 0.88.

3.5. Detection limits

The limit of detection (lod; mlod), of α-quartz from NIST SRM 1878a samples was estimated using the 3-σ criterion, defined by the international union of pure and applied chemistry (IUPAC) (Boqué and Rius, 1996), as,

$$m_{lod} = 3\sigma / S_m \quad (1)$$

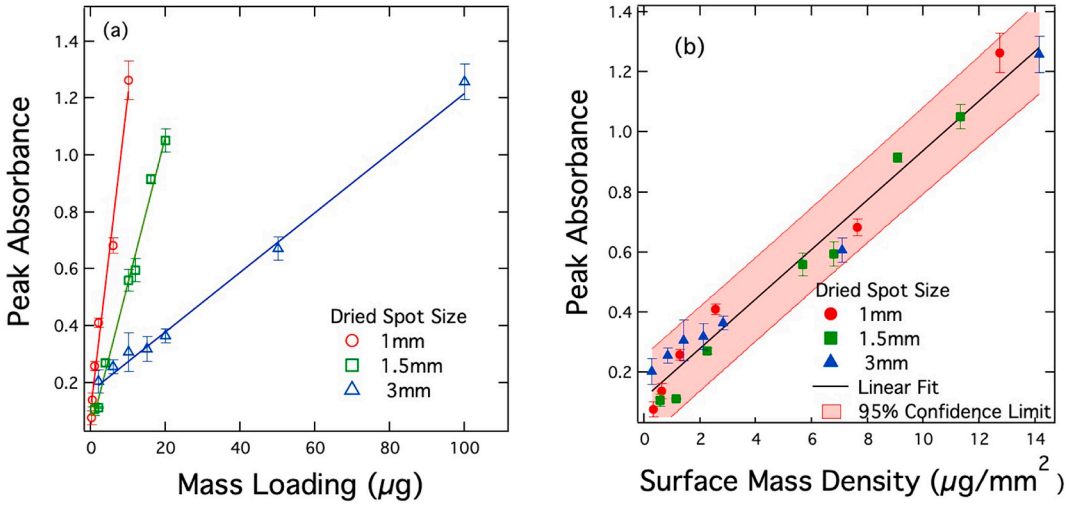

Fig. 4. (a) Calibration curves constructed by plotting peak absorbance at 798 cm^{-1} as a function of mass per filter for three dried spots (1, 1.5, and 3 mm diameter); (b) Measured peak absorbance as a function of surface mass density (mass per unit area of the dried spot). The lines represent linear fits to the experimental data.

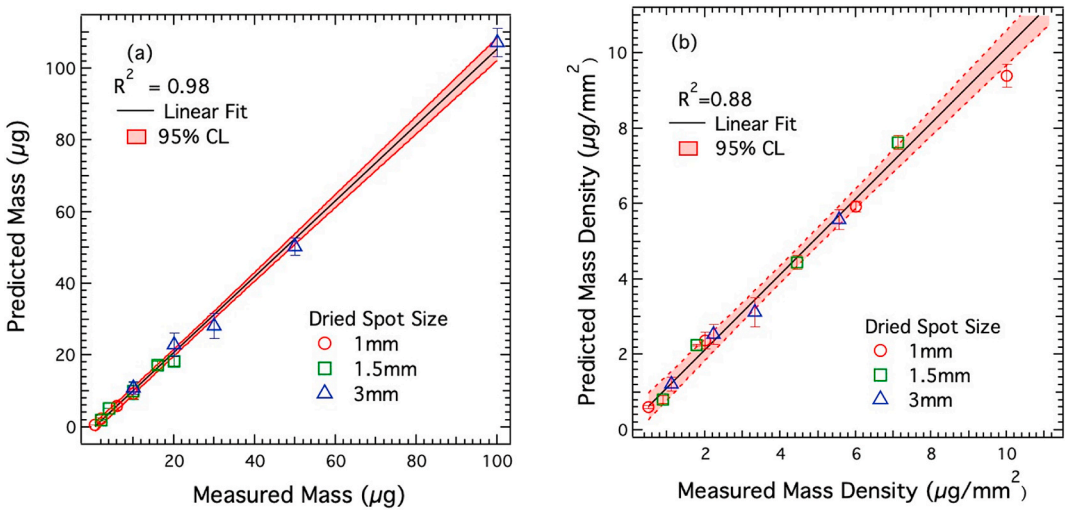

Fig. 5. Performance of the PLS model for three spot sizes: (a) Predicted vs measured mass loading (in μg) of α-quartz per filter obtained using PLS models constructed for three dried spot diameters; (b) Predicted vs measured mass density (mass of α-quartz per unit area of spot; in μg/mm^2). The lines represent linear fits to the experimental data.

For univariate calibration, S_m is the slope of the calibration curve. For multivariate calibration, the LOD is obtained using the following equation (Boqué & Rius, 1996; Valderrama et al., 2007):

$$m_{lod} = 3.3\sigma/_{S_m} = 3.3\sigma b = 3.3\sigma\sqrt{(b_1^2 + \cdots b_n^2)} \quad (2)$$

where σ is the standard deviation of QCL-IR spectra obtained for the blank filters in the wavenumber range 750–1030 cm−1, which represents the background signal noise; S_m is the measurement sensitivity in terms of analyte mass; b is the Euclidian norm of the regression coefficient vector; and b_n is the n^{th} regression coefficient. S_m is estimated as the inverse of b. The standard deviation of the noise from the blank filters was calculated from the spectra in the range 766–842 cm−1.

Method detection limits were determined both using univariate peak height and the PLS model. According to Eq. (1), for univariate

Table 2
Comparison of various analytical methods used for airborne crystalline silica quantification that involve filter pretreatment.

Method	Analytical Technique	Filter Pre-treatment	Sample Preparation	Collection Media	Mass LOD, μg	LOD*, Air Concentration, μg m^{-3}
This study	QCL-IR	Low-temperature plasma ashing	Resuspension and redeposition as a dried spot of 1–3 mm diameter	MCE filter for aerosol collection; PC filter for redeposition	0.39–1.94	0.41–2.0
NIOSH 7602 (NIOSH, 2017b)	FTIR	Low-temperature plasma ashing	Mix with KBr, press into 13-mm pellet	PVC filters	5	5.2
NIOSH 7603 (NIOSH, 2017a)	FTIR	Low-temperature plasma ashing;	Resuspend and redeposit on half of vinyl/acrylic co-polymer filter (DM-450) filters	PVC filters for collection; DM-450 filters for redeposition	10	10.4
MSHA P-7 (MSHA, 2013)	FTIR	Low-temperature plasma ashing;	Resuspend and redeposit on 9 mm diameter area of DM-450 filters	PVC filters for collection; DM-450 filters for redeposition	4	4.2
MSHA P-2 (MSHA, 1999)	XRD	Low-temperature plasma ashing	Resuspend and redeposit on 25 mm silver filters	PVC for collection; silver filters for redeposition	5	5.2
OSHA ID-142 (Esswein et al., 2013)	XRD	Tetrahydrofuran (THF) digestion	Resuspend and redeposit on 25 mm silver filters	PVC for collection; silver filters for redeposition	2.84	2.9
Zheng et al. (2018)	Raman	Low-temperature plasma ashing	Resuspend and redeposit as 1–3 mm diameter dried spot	MCE filter for collection; Silver filters for redeposition	0.055–3.2	0.06–3.1
Stacey, Clegg, Morton, and Sammon (2020)	Raman	Low-temperature plasma ashing	Redeposition on 10-mm filters	Silver membrane filters for collection or redeposition	0.26	0.27

method, the detection limits are 0.15 μg, 0.24 μg and 1.14 μg, while for multivariate method, the detection limits for α-quartz were determined to be 0.12 μg, 0.22 μg, and 1.04 μg for spot diameters of 1 mm, 1.5 mm, and 3 mm, respectively. The LODs results are match well between univariate and multivariate methods. These values are significantly lower than LODs reported for both conventional XRD and FTIR methods involving filter pretreatment (NIOSH, 2003a, 2003b; 2017b). Table 2 summarizes the current methods that are used to measure α-quartz using different techniques. The LODs for the QCL method are generally an order of magnitude lower than those of the currently used standard methods.

3.6. Measurement of workplace aerosol samples

The QCL-IR method described above was extended to aerosol samples obtained from workplaces, as described above. Various organic and/or inorganic components of the sampled particulate matter can potentially interfere with the IR measurement. Aerosol samples collected at construction sites may contain organic components from man-made polymer composite products. IR measurement of airborne dust generated in coal mines is often subject to particulate mineral interferants (Yassin et al., 2005).

Many bituminous coal aerosols contain kaolinite, a common interfering mineral (ASTM, 2014). Some polymorphs of crystalline silica such as cristobalite and tridymite, which are less common in workplace aerosols, could also potentially interfere with α-quartz measurement (ASTM, 2014;NIOSH, 2003a, 2003b; NIOSH, 2017a, 2017b). Cristobalite absorbs at the same peak frequency as α-quartz and therefore interferes positively; however, cristobalite is not found in coal mine dusts. Tridymite is very rare and its absorption peak can be resolved from the other two polymorphs. Even with potential interference from the other polymorphs, the QCL-IR method can still provide meaningful 'total' RCS (as α-quartz plus cristobalite) quantification for compliance measurement, because the current OSHA PEL is not specific to a polymorph.

Other sources of spectral interference from contaminants in the workplace air, such as diesel particulate matter or other organic aerosol, can also be significant in some workplaces. However, the filter pretreatment involving plasma ashing minimizes such organic interferences (NIOSH, 2017a, 2017b).

QCL-IR measurements were obtained for all three representative workplace samples. QCL measurements from these samples were compared with XRD results from the reference NIOSH Method 7601 (NIOSH, 2003a, 2003b). Test aerosols with relatively high air concentrations of α-quartz were collected for 2 min at 1.2 L·min^{-1} for the QCL-IR method, and for 10 min at 2 L·min^{-1} for the XRD method. For measuring low concentration aerosols, the collection time was 10 min for the QCL-IR method, and 2 h for the reference XRD method. The concentrations of α-quartz in the test aerosols were in the range 30–4000 μg·m^{-3}. Aerosol samples with α-quartz concentrations below 30 μg·m^{-3} were not tested because their mass loading obtained over a 2-h sampling time would be below the limit of quantitation (LOQ) of the reference XRD method (NIOSH, 2003a, 2003b).

QCL-IR spectra of sample ST and sample FC at various mass loadings showed the characteristic peaks at 798 cm^{-1} and confirm the presence of α-quartz in both sample matrices, as shown in Fig. 6. The α-quartz content of each sample was determined using both univariate and multivariate calibration methods, as described above.

Comparisons of RCS mass per filter obtained from QCL-IR and XRD methods for an aerosol with the same air concentration of RCS (for each sample) are shown in Table 3. Different sample collection times for the QCL-IR and the XRD methods had to be used because of significant differences in the LODs of these methods. The LOD of the XRD method was 5 μg while that of the QCL-IR method was in the range 0.12–1.14 μg for different dried spot sizes used. The lowest mass loadings used to test the QCL-IR method in our study ranged from 0.5 to 0.7 μg. For the test aerosol concentration and sampling flow rates used in our experiments, a minimum collection time of 1.5 min was adequate to measure α-quartz above the limit of quantification (LOQ) using the QCL-IR method. In contrast, sample

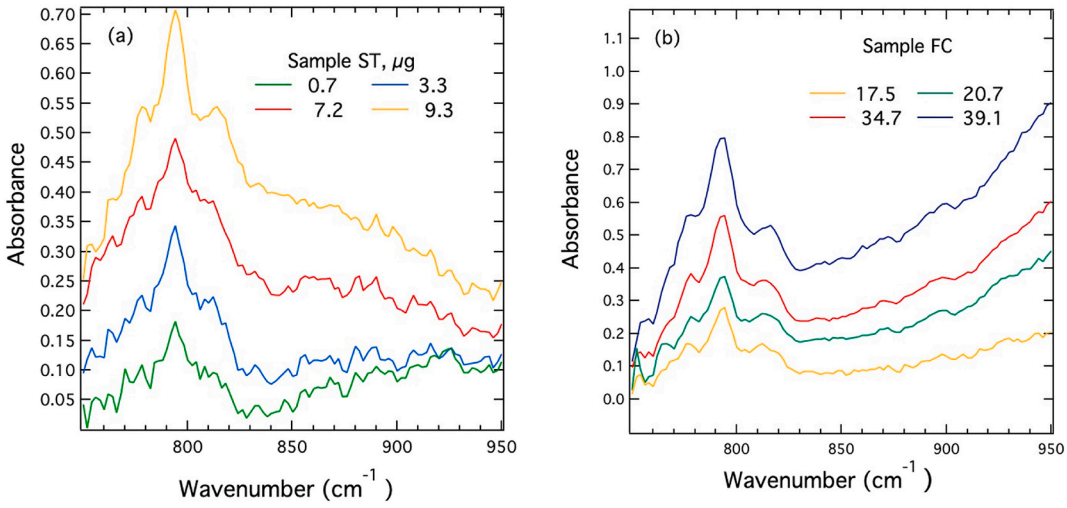

Fig. 6. (a) QCL-IR spectra of engineered stone sample ST (after filter pretreatment) at various concentrations; (b) QCL-IR spectra of fiber cement siding (FC) samples with various mass loadings (obtained by the univariate method).

collection times of 10–120 min were needed for measurement above LOQ of the XRD method.

Air concentrations of RCS, corresponding to mass per filter in Table 3, for each of the four samples are shown in Fig. 7(a) and (b). Linear regression best fits to both univariate and multivariate data in Fig. 7 are included in the Supplemental Information (SI). These best fits show excellent correlation between QCL-IR and XRD measurements, with coefficient of determination (R^2) in the range 97–99%. The slope of the linear fit was 0.86 using univariate and 0.76 using multivariate calibration for engineered stone samples (ST), showing 15–25% underestimation of crystalline silica concentrations. Univariate calibration leads to lesser deviation from the XRD method. The reasons for this underestimation are not known; we surmise they could be related to either larger size of particles in the ST sample (dissimilarly affecting the QCL and XRD measurements) or to the large difference in the sample mass analyzed by the two methods. However, in contrast, the samples FC and the sample CD (discussed below) showed excellent agreement, with their regression slopes being very close to 1 (within 1–3%). In general, these results show good agreement between the two methods (for the samples studied in this work), particularly considering that the total mass loading on the filter for the QCL-IR was an order of magnitude lower compared to that for the XRD method.

Two-factor analysis of variance (ANOVA) with replication was applied to further probe the statistical differences between the QCL-IR method (for both univariate and multivariate calibration approaches) and the standard XRD method. ANOVA of airborne α-quartz concentrations from sample ST showed no statistically significant differences between the three methods: QCL-IR (univariate), QCL-IR (multivariate), and the standard XRD method ($F(2, 16) = 0.96$, $p > 0.05$). For sample ST, the univariate approach provided slightly better agreement with the XRD method, with the deviation ranging from 6 to 26% for the four samples. For the aerosol from sample FC, the ANOVA analysis did not show statistically significant differences between the three methods ($F(2, 16) = 0.30$, $p > 0.05$). For this sample, both univariate and multivariate methods provided similar results, with estimates differing by 3–14% compared to the XRD method.

3.7. Correction for kaolinite interference in coal samples

Kaolinite has a characteristic peak at 800 cm^{-1}, completely overlapping the α-quartz peak at 798 cm^{-1}. The presence of kaolinite, if not corrected for, leads to overestimation of α-quartz mass. The methods NIOSH 7603 ((NIOSH), 2017a) and MSHA P-7 ((MSHA), 2013) use a spectral correction approach involving measurement of the absorption peak of kaolinite at 920 cm^{-1}, where there is no quartz IR peak. Fig. 8(a) shows the characteristic peaks of α-quartz and kaolinite as measured by QCL-IR. Both α-quartz and kaolinite show peak absorbance at 798 cm^{-1}; however, only kaolinite shows peak absorbance at 920 cm^{-1}. The correction approach involves using the ratio of the two kaolinite peak absorbance at 920 and 798 cm^{-1}. Using this *a priori* known ratio and the peak absorbance at 920 cm^{-1} of an unknown sample, the contribution of kaolinite to the absorbance at 798 cm^{-1} is estimated ((MSHA), 2013; (NIOSH), 2017a). The absorbance corresponding to α-quartz at 798 cm^{-1} can then be obtained by subtracting the kaolinite signal from the total absorbance at that frequency.

QCL-IR spectra of kaolinite with different mass loadings are shown in Fig. 8(b). The absorbance of kaolinite at 920 cm^{-1} decreases with increasing mass loading. The spectral contribution of kaolinite at 798 cm^{-1} is obtained as (Yassin et al., 2005):

$$A_{798} = \frac{A_{920}}{f_c} \tag{4}$$

where the A_{798} is the absorbance of kaolinite at 798 cm^{-1} and A_{920} is the absorbance of kaolinite at 920 cm^{-1}. The value f_c is correction factor, which is defined as the slope of the regression line for the ratio of kaolinite absorbance at 920 cm^{-1} to that at 798 cm^{-1}.

The univariate approach based on peak height was used for the construction of calibration curves for kaolinite. In Fig. 9, the calibration curve based on the peak height at 920 cm^{-1} used a linear baseline between 900 cm^{-1} to 942 cm^{-1} to calculate peak height; R^2 of the linear regression was 0.98. The ratio of the two characteristic kaolinite absorbance at 920 cm^{-1} and 798 cm^{-1} at various mass loadings (T_{920}/T_{798}) was practically constant at 1.7 at all kaolinite masses examined. Therefore, by calculating the peak height absorbance of kaolinite at 920 cm^{-1}, the contribution of the absorbance of kaolinite at 798 cm^{-1} can be measured accurately.

For constructing a partial least squares (PLS) model, the absorbance data between wavenumber range 906–940 cm^{-1} were selected

Table 3
RCS content in workplace samples measured by QCL-IR and XRD methods, corresponding to equivalent air concentration for each sample shown in Fig. 7(a)–(b).

	Sample #	QCL-IR method (univariate)	QCL-IR method (multivariate)	XRD method[a]
		Mass per filter, μg	Mass per filter, μg	Mass per filter, μg
Sample **ST**	1	0.7	0.5	7.8
	2	3.3	4.4	25
	3	7.2	6.9	33
	4	9.4	11.1	79
Sample **FC**	1	17.5	18.0	20
	2	20.7	20.4	20
	3	34.8	29.1	68
	4	39.1	39.5	115

[a] The sample collection time was much larger compared to that for the QCL method to obtain enough particulate mass above LOQ.

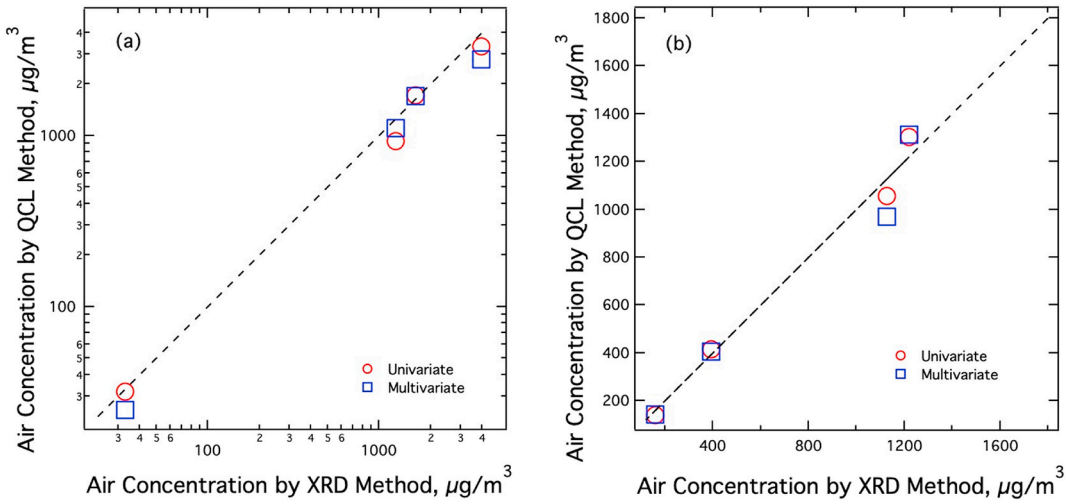

Fig. 7. Comparison of air concentration of α-quartz measured using QCL-IR methods with the reference XRD method for two types of aerosol: (a) engineered stone sample ST, and (b) fiber cement siding sample FC. Corresponding filter loadings (mass per filter) are shown in Table 3. The dotted curve is a 1:1 line. The linear regression fits to these data are provided in Supplemental Information.

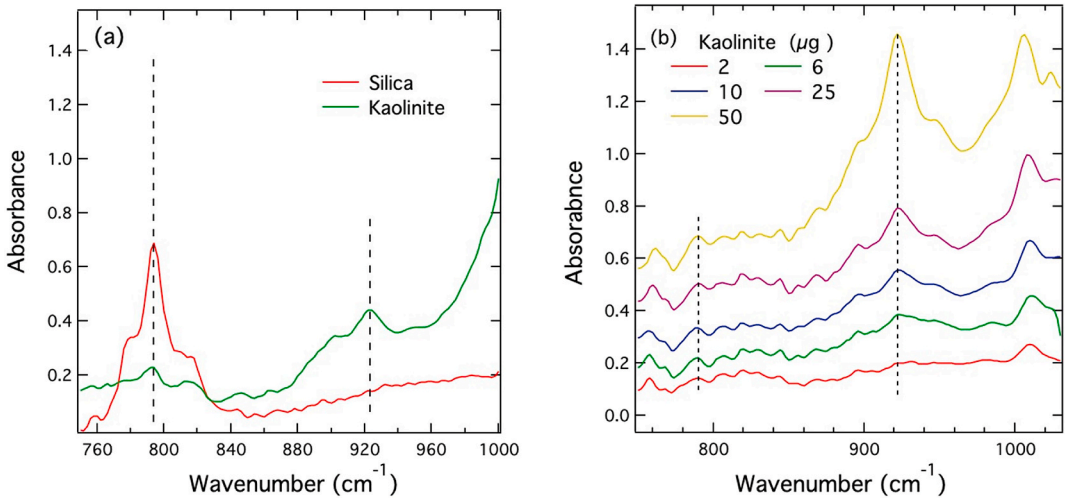

Fig. 8. (a) Comparison of QCL-IR spectra of standard reference α-quartz and kaolinite; (b) QCL-IR spectra of samples with various kaolinite mass loadings per filter prepared using syringe filtration.

as X variables, while 24 filter samples with mass loadings ranging from 2 to 50 μg were used as Y variables. As seen in Fig. 10, using the PLS model, all predicted mass loadings were within the 95% confidence limit; the regression coefficient R^2 was 0.95.

Fig. 11 shows the spectra obtained for unknown aerosols from prepared sample CD containing coal dust. Both characteristic peaks of α-quartz and kaolinite at 798 cm^{-1} and 920 cm^{-1} are visible in the spectra. The peak absorbance at 920 cm^{-1} indicates the presence of kaolinite in sample CD. The correction for kaolinite was applied to calculation of the peak height for α-quartz at 798 cm^{-1}. Univariate calibration was used for predicting the α-quartz content in the sample CD.

Fig. 12 shows the air concentration of four types of coal mine samples. Each sample type was measured using three methods: the univariate method (after correction for kaolinite), the multivariate method (using the PLS model), both by QCL-IR, and by the XRD method. Linear best fits to these data are provided in SI, showing excellent correlation. The slope of the linear regression was 0.97 for univariate calibration and 1.02 for multivariate calibration.

The filter loadings (mass per filter), of kaolinite and α-quartz in the coal mine dust samples are shown in Table 4. To reiterate, the values are based on the average of at least three samples collected under the same conditions. After correction for kaolinite interference, the α-quartz content using the QCL-IR method for all the samples agree well with the results from the XRD method, as shown in Table 4. ANOVA of airborne α-quartz mass loadings in sample CD showed no statistically significant difference between the QCL-IR and the XRD method ($F(1, 16) = 0.95$, $p > 0.05$).

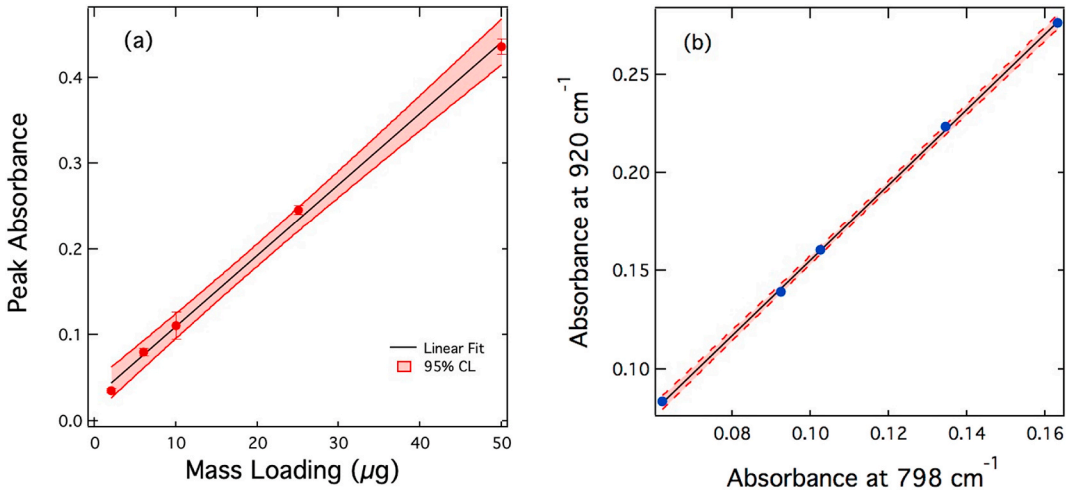

Fig. 9. (a) Calibration curve for kaolinite using peak height at 920 cm^{-1}. (b) A linear regression showing the relationship between the kaolinite absorbance at 798 cm^{-1} and 920 cm^{-1}. The black solid line shows a linear fit.

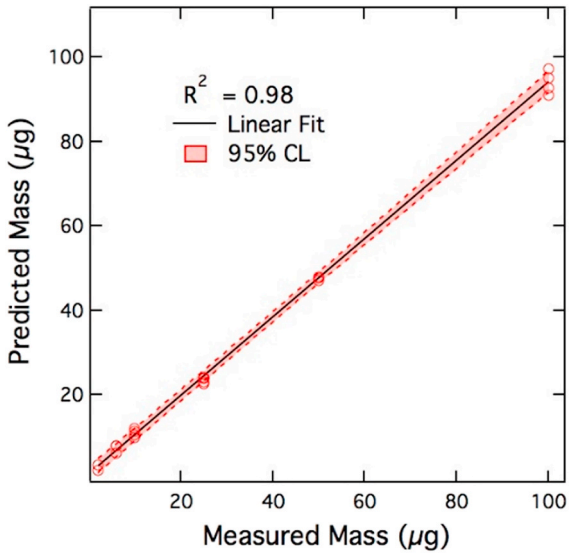

Fig. 10. PLS model performance: predicted vs measured kaolinite mass loading per filter.

4. Conclusions

The QCL-IR transmittance measurement scheme was successfully applied to the determination of particulate crystalline silica in workplace atmospheres. QCL measurements of RCS were carried out on realistic workplace aerosol sample matrices for the first time. Dried sample spots, obtained from redeposition of the ashed particulate samples, were optimally coupled with the QCL beam to improve the detection limits. The LOD of the method ranged from 0.12 to 1.14 μg, for dried sample spot diameters in the range 1–3 mm, respectively. These LODs are notably lower than those of the established standard methods, which range from ~3 to 10 μg.

The QCL method was evaluated using three types of representative workplace aerosol samples with distinct particle matrices. The concentrations obtained using univariate as well as multivariate calibration approaches agreed within 3–26% of the measurements from a standard XRD method for most samples. The scheme used to correct for kaolinite interference in CD samples yielded α-quartz measurements that agreed well with the results from the XRD method.

Due to small suspension volumes and syringe filtration, the dried spot preparation method described here is substantially simpler than the KBr pellet preparation required for standard FTIR methods as well as the filter redeposition techniques used in other XRD and FTIR methods. The overall simplicity, robustness, and compact nature of QCL-based spectrometers makes this method a suitable alternative to current standard methods for measurement of RCS. And, most importantly, the method detection limit of the QCL method is at least an order of magnitude better than LODs of the standardized XRD and FTIR methodologies.

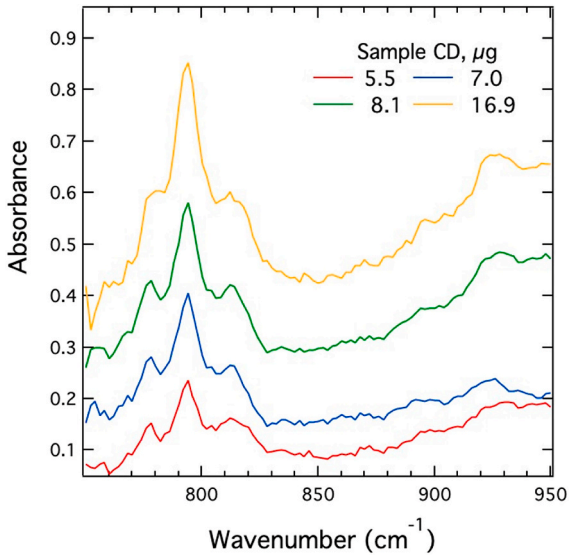

Fig. 11. QCL-IR spectra of coal dust sample CD with various mass loadings per filter after pre-treatment.

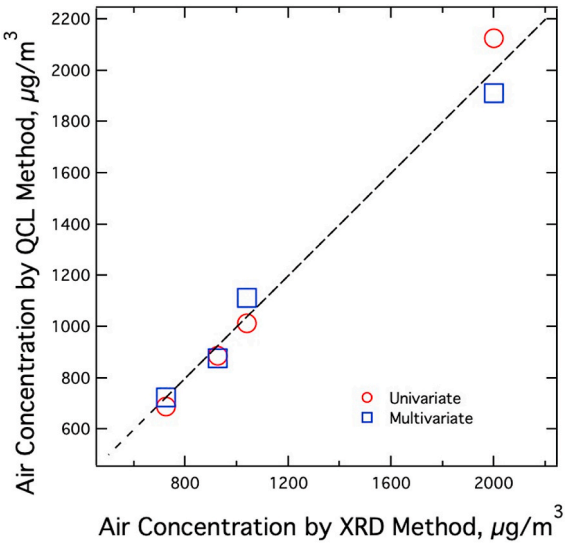

Fig. 12. Comparison of air concentration of α-quartz measured using QCL and XRD methods for various coal dust samples. The corresponding filter loadings (mass per filter) are shown in Table 4. The dotted curve is a 1:1 line. The linear regression fits to these data are provided in Supplemental Information.

Table 4
Comparison of respirable α-quartz content per filter obtained using QCL-IR and XRD methods for four coal dust (CD) samples, corresponding to equivalent air concentration for each sample shown in Fig. 12.

Sample #	QCL method		XRD method
	Kaolinite content, μg	α-quartz content, μg	α-quartz content, μg
1	5.5	5.8	5.8
2	7.1	7.0	7.4
3	8.1	8.9	8.3
4	17.0	15.3	16

Further studies will be needed to assess more meaningful analytical figures of merit for a broad range of real-world crystalline silica aerosols. While the limited number of sample types used in this study may not allow predicting the overall method performance, it is worth noting that infrared absorption spectroscopy using FTIR has been widely used for analysis of crystalline silica in workplace aerosols. In this respect, the QCL approach presented in this work shares similar spectroscopic features and limitations of the FTIR method with respect to matrix and mineral interferences. The study demonstrates that the QCL-IR method can provide precision and accuracy comparable to those of the traditional XRD or FTIR methods.

Declaration of Competing Interest

The authors declare that they have no known competing financial interests or personal relationships that could have appeared to influence the work reported in this paper.

Acknowledgements

The authors would like to thank Mr. Gregory Deye and Dr. Chaolong Qi for help with crystalline silica sample preparation and Drs. Rosa Key-Schwartz, Taekhee Lee and Robert Streicher for helpful feedback. This work was supported by a NIOSH National Occupational Research Agenda (NORA) intramural grant (CAN#939051U).

Appendix A. Supplementary data

Supplementary data related to this article can be found at https://doi.org/10.1016/j.jaerosci.2020.105643.

References

ASTM International (American Society for Testing and Materials). (2014). *ASTM D7948 - 14: Standard test method for measurement of respirable crystalline Silica in workplace air by infrared spectrometry*. West Conshohocken: ASTM International (American Society for Testing and Materials). https://doi.org/10.1520/D7948-14.

Boqué, R., & Rius, F. X. (1996). Multivariate detection limits estimators. *Chemometrics and Intelligent Laboratory Systems, 32*(1), 11–23. https://doi.org/10.1016/0169-7439(95)00049-6.

Esswein, E. J., Breitenstein, M., Snawder, J., Kiefer, M., & Sieber, W. K. (2013). Occupational exposures to respirable crystalline silica during hydraulic fracturing. *Journal of Occupational and Environmental Hygiene, 10*(7), 347–356.

HSE. (2014). *Methods for the Determination of Hazardous Substances, MDHS 101/2. Crystalline silica in respirable airborne dusts: Direct on-filter analyses by infrared spectroscopy and X-ray diffraction* (pp. 1–21). UK: Health and Safety Executive.

IFA. (2018). *GESTIS Database: International limit values for chemical agents (occupational exposure limits). Sankt Augustin*. Germany: IFA.

International Organization for Standardization. (2015). *ISO 16258: Workplace air – analysis of respirable crystalline silica by X-ray diffraction (2 parts)*. Geneva, Switzerland.

Lee, R. J., Van Orden, D. R., Cox, L. A., Arlauckas, S., & Kautz, R. J. (2016). Impact of muffle furnace preparation on the results of crystalline silica analysis. *Regulatory Toxicology and Pharmacology, 80*, 164–172. https://doi.org/10.1016/j.yrtph.2016.06.002.

MSHA. (1999). *X-ray diffraction determination of quartz and cristobalite in respirable mine dust: Method P-2*. Pittsburgh, PA: U.S. Department of Labor, Mine Safety and Health Administration.

MSHA. (2013). *Infrared determination of quartz in respirable coal mine dust: Method P-7*. Pittsburgh, PA: U.S. Department of Labor, Mine Safety and Health Administration.

NIOSH. (2003a). Silica, crystalline, by XRD (filter redeposition): Method 7500. *NIOSH Manual of Analytical Methods, 4*, 4th ed.

NIOSH. (2003b). Silica, crystalline, by VIS, method 7601. NIOSH man. In *Anal. Methods*. Cincinnati, OH: DHHS NIOSH Publ.

Occupational Safety and Health Administration (OSHA). (2016). Occupational exposure to respirable crystalline silica: Final rule. *Federal Register, 81*(58), 16285–16890.

NIOSH. (2017a). Quartz in respirable coal mine dust, by IR (redeposition): Method 7603. *NIOSH Manual of Analytical Methods, 3*, 5th ed.

NIOSH. (2017b). Silica, respirable crystalline, by IR (kbr pellet): Method 7602. *NIOSH Manual of Analytical Methods, 4*, 5th ed.

Stacey, P., Clegg, F., Morton, J., & Sammon, C. (2020). An indirect Raman spectroscopy method for the quantitative measurement of respirable crystalline silica collected on filters inside respiratory equipment. [10.1039/D0AY00165A]. *Analytical Methods, 12*(21), 2757–2771. https://doi.org/10.1039/D0AY00165A.

Valderrama, P., Braga, J. W. B., & Poppi, R. J. (2007). Variable selection, outlier detection, and figures of merit estimation in a partial least-squares regression multivariate calibration model. A case study for the determination of quality parameters in the alcohol industry by near-infrared spectroscopy. *Journal of Agricultural and Food Chemistry, 55*(21), 8331–8338. https://doi.org/10.1021/jf071538s.

Wei, S., Kulkarni, P., Ashley, K., & Zheng, L. (2017). Measurement of crystalline silica aerosol using quantum cascade laser–based infrared spectroscopy. *Scientific Reports, 7*(1), 13860.

Yassin, A., Yebesi, F., & Tingle, R. (2005). Occupational exposure to crystalline silica dust in the United States, 1988–2003. *Environmental Health Perspectives, 113*(3), 255–260. https://doi.org/10.1289/ehp.7384.

Zheng, L., Kulkarni, P., Birch, M. E., Ashley, K., & Wei, S. (2018). Analysis of crystalline silica aerosol using portable Raman spectrometry: Feasibility of near real-time measurement. *Analytical Chemistry, 90*(10), 6229–6239. https://doi.org/10.1021/acs.analchem.8b00830.